Scripta METALLURGICA et MATERIALIA
Vol. 24, pp. 2309-2314, 1990
Printed in the U.S.A.

CYCLIC STRAIN LOCALIZATION IN ION BEAM MICROALLOYED NICKEL

D.J. Morrison†, J.W. Jones+, and G.S. Was*
†Department of Mechanical and Aeronautical Engineering, Clarkson University, Potsdam, NY 13699, +Department of Materials Science and Engineering and *Department of Nuclear Engineering, The University of Michigan, Ann Arbor, MI 48109

(Received August 28, 1990)
(Revised September 24, 1990)

Introduction

During cyclic deformation, many metals exhibit localization of plastic strain in persistent slip bands (psbs) (1). Fatigue cracks may initiate where the psbs intersect the surface. Numerous studies have established that the emergence of psb features at the surface can be significantly suppressed by the use of surface modification techniques such as ion beam microalloying (2,3). The modifications may alter the strength, elastic modulus, stacking fault energy, and residual stress state of the surface (4). As a result, the properties of the surface region can differ significantly from the properties of the subsurface. Even though the evolution of surface psb features can be significantly affected by a surface modification, the question remains as to the effect of a surface modification on bulk cyclic deformation mechanisms. Prior studies have concentrated on the effects of the modifications on cyclic hardening. The results of these studies have been inconclusive. Studies on copper single crystals indicated in one case (5) that ion beam surface modifications increased cyclic flow stress, while in another case (6) no change in cyclic flow stress was observed. Similar work on polycrystals has been somewhat mixed with one study (7) indicating that surface modifications decrease cyclic flow stress and another study (8) reporting that surface modifications had no effect on cyclic flow stress.

It has been demonstrated in single crystal copper (9-11) and nickel (12) that the localization of plastic strain in psbs causes significant changes in the shape of the stress-strain hysteresis loop. Specifically, strain localization and the concurrent formation of psbs lead to a more parallelogram-shaped hysteresis loop. Recent studies have shown that this phenomenon is also exhibited in polycrystalline materials (13,14). The loop shape change can be measured by computing the loop shape parameter, V_H, which is defined as the area enclosed by the hysteresis loop divided by the area of the parallelogram that circumscribes the loop as shown in Figure 1. The objective of this study was to use hysteresis loop shape analysis and cyclic hardening comparisons to determine the effect of ion beam surface microalloying on bulk strain localization in cyclically deformed polycrystalline nickel.

Experimental Procedures

Cylindrical fatigue specimens as shown in Figure 2 were machined from Ni-270 (99.98% Ni) rods. The specimens were annealed in an atmosphere of flowing argon-3% hydrogen for 4 hours at 1000°C resulting in a microstructure with an average lineal grain boundary intercept of 290 μm. The gage sections were electropolished in a solution of ethanol-20% perchloric acid at -50°C.

One specimen received a surface modification that consisted of first evaporating alternating layers of nickel and aluminum onto the gage section in an electron beam evaporation chamber

0036-9748/90 $3.00 + .00

operating at a base pressure of 6.6×10^{-5} Pa. Three nickel layers, each 6 nm thick, and two aluminum layers, each 41 nm thick, were applied. This multilayer structure was then ion beam mixed with 3 MeV Ni^{++} ions to a dose of 1×10^{16} ions/cm^2 to achieve a homogeneous composition of Ni-75 at.% Al in the near-surface region. The ion irradiation was performed in a General Ionex 1.7 MV tandem ion accelerator operating at a vacuum better than 5.3×10^{-6} Pa. A beam current of 2 μA heated the specimen to 220°C during ion beam mixing. The specimen was continuously rotated at 20 rpm during all evaporations and ion beam mixing processes to ensure uniform modification over the entire surface of the gage section.

Cyclic deformation experiments were conducted at room temperature using a servo-hydraulic fatigue testing system. Specimens were cycled under fully-reversed tension/compression at a constant plastic strain amplitude (ε_p) of 2.5×10^{-4}. Prior to saturation, the specimens were cycled using a triangular waveform at a constant total strain rate of 2.0×10^{-3}/s. After saturation the total strain rate was increased to 4.0×10^{-2}/s. Hysteresis loops were periodically recorded at a total strain rate of 2.0×10^{-4}/s. The different strain rates did not appear to affect the stress-strain response. Acetate replicas of the surfaces were obtained to provide a record of the evolution of slip features.

Results and Discussion

Micrographs shown in Figure 3 depict the surfaces of the unmodified and surface modified specimens after 4000 and 40,000 fatigue cycles. After 4000 cycles, numerous psbs are clearly seen at the surface of the unmodified specimen. However, the modified specimen exhibits almost no evidence of psb activity at the surface. After 40,000 cycles the psb density in the unmodified specimen has increased and some psbs are now seen at the surface of the modified specimen.

Cyclic hardening and V_H curves for the unmodified and surface modified specimens are shown in Figures 4(a) and (b). In these figures stress amplitude (σ_a) and V_H are plotted as functions of cumulative plastic strain ($\varepsilon_{p,cum}$) which is defined as $4\varepsilon_p N$ where N is the number of cycles. Cyclic hardening behavior up to the saturation point can be characterized by the equation

$$\sigma_a = \sigma_m - (\sigma_m - \sigma_o) \exp(-R\, \varepsilon_{p,cum})$$

where σ_m is the maximum stress amplitude, σ_o is the stress amplitude after the first quarter cycle, and R is an empirically determined constant related to the hardening rate (15). An analysis of the cyclic hardening curves produces the values shown in Table I. The similarity of these values indicates that the surface modification had little influence on bulk cyclic hardening. Some variation in σ_o would be expected due to the very low initial strength of the material and the number of processing steps required prior to the first fatigue cycle. The decrease in σ_a near the end of each cyclic hardening curve was caused by the initiation and growth of fatigue cracks. Although crack initiation and fatigue life are not the primary focus of this paper, it can be seen from the drop in σ_a that the surface modification delayed crack initiation by a modest amount.

TABLE I

Cyclic Hardening Parameters

	σ_m (MPa)	σ_o (MPa)	R
Unmodified	158	8	0.697
Modified	159	11	0.679

The correlation between V_H and the formation of psbs in the unmodified specimen is shown in Figure 5. In this figure V_H and the percentage of the surface area covered by psbs (psb area fraction) are plotted as functions of $\varepsilon_{p,cum}$. It is seen that the two curves parallel each other very closely, and the abrupt increase in V_H when $\varepsilon_{p,cum} \approx 2$ corresponds with the beginning of the formation of psbs. The V_H curves for the unmodified and modified specimens can be compared in Figures 4(a) and (b). These figures show that both types of specimens demonstrated similar hysteresis loop shapes. Prior to cyclic saturation, V_H for both specimens was 0.67. The value of V_H increased to 0.76 after saturation. Therefore, although the surface modification significantly suppressed the emergence of psbs at the surface, psbs formed in the subsurface region of the modified specimen in the same manner as in the unmodified specimen.

Conclusions

The present work, in agreement with the recent findings of Polak et al. (14), shows that loop shape parameter measurements can be successfully used in polycrystals to determine the onset of strain localization resulting from bulk psb formation. Furthermore, based on the similarity of the cyclic hardening and loop shape parameter curves, it can be concluded that the same fundamental cyclic deformation mechanisms are operating in the bulk of the unmodified and surface modified specimens. These results agree with findings of other studies which were based on surface removal experiments (16) and TEM observations of subsurface dislocation structures (17).

Acknowledgments

This research was supported by the National Science Foundation through grant DMR-8603174. Surface modifications were performed at the Michigan Ion Beam Laboratory for Surface Modification and Analysis at the University of Michigan.

References

1. C. Laird, P. Charsley, and H. Mughrabi, Mater. Sci. Eng., 81, 433-450 (1986).
2. R. G. Vardiman, in Ion Plating and Implantation Applications to Materials, R. F. Hochman, Ed., American Society for Metals, 1986, pp.107-113.
3. D. S. Grummon, J. W. Jones, and G. S. Was, Metall. Trans. A, 19A, 2775-2787 (1988).
4. D. J. Morrison, J. W. Jones, G. S. Was, A. Mashayekhi, and D. W. Hoffman, in Materials Research Society Symposium Proceedings. Volume 130, J. C. Bravman, W. D. Nix, D. M. Barnett, and D. A. Smith, Eds., Materials Research Society, 1989, pp.53-58.
5. J. Mendez, P. Villechaise, and P. Violan, in Strength of Metals and Alloys. Proceedings of the 8th International Conference, P. Kettunen, T. K. Lepisto, and M. E. Lehtonen, Eds., Pergamon Press, Oxford, 1988, pp. 737-742.
6. E. Y. Chen and E. A. Starke, Mater. Sci. Eng., 24, 209-221 (1976).
7. A. Kujore, S. B. Chakrabortty, E. A. Starke, and K. O. Legg, Nucl. Instrum. and Methods, 182/183, 949-958 (1981).
8. J. Mendez, P. Violan and M. F. Denanot, Nucl. Instrum. and Methods in Phys. Res., B19/20, 232-235 (1987).
9. H. Mughrabi, Mater. Sci. Eng., 33, 207-223 (1978).
10. A. Abel, Mater. Sci. Eng., 36, 117-124 (1978).
11. J. Polak, J. Helesic, and K. Obrtlik, Mater. Sci. Eng. A, 101, 7-12, (1988)
12. C. Blochwitz and U. Veit, Crystal Res. and Technol., 17, 529-551 (1982).

13. D. J. Morrison, PhD. Dissertation, The University of Michigan (1989).
14. J. Polak, J. Helesic, and K. Obrtlik, Scripta Metall., 24, 415-420 (1990).
15. D. L. Anton and M. E. Fine, Metall. Trans. A, 13A, 1187-1198 (1982).
16. D. S. Grummon, D. J. Morrison, J. W. Jones, and G. S. Was, Mater. Sci. Eng. A, 115, 331 (1989).
17. D. J. Morrison, J. W. Jones, D. E. Alexander, and G. S. Was, Metall. Trans. A (in press).

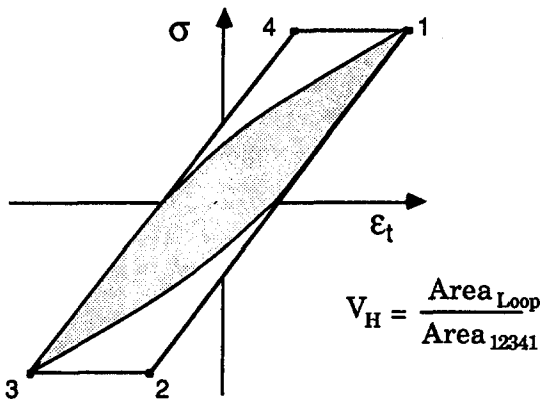

FIG. 1. Areas used to calculate the hysteresis loop shape parameter, V_H. The loop shape parameter is equal to the area enclosed by the loop divided by the area of the parallelogram that circumscribes the loop.

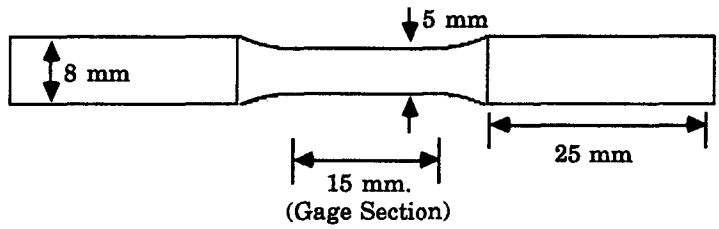

FIG. 2. Nickel-270 axial fatigue specimen geometry.

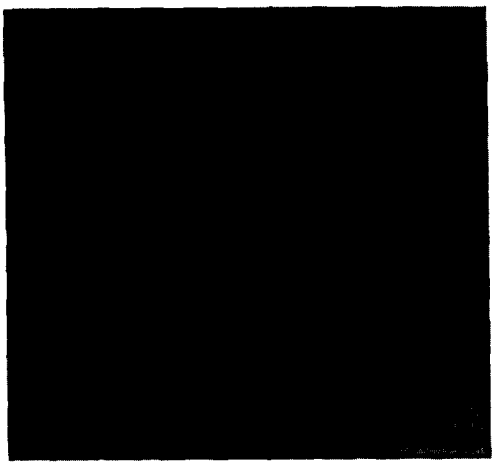

(a) Unmodified - 4000 cycles

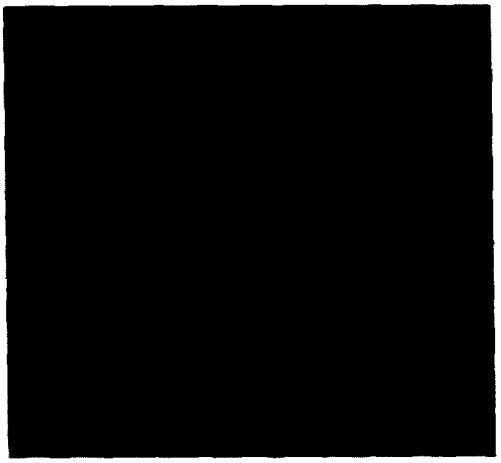

(b) Unmodified - 40,000 cycles

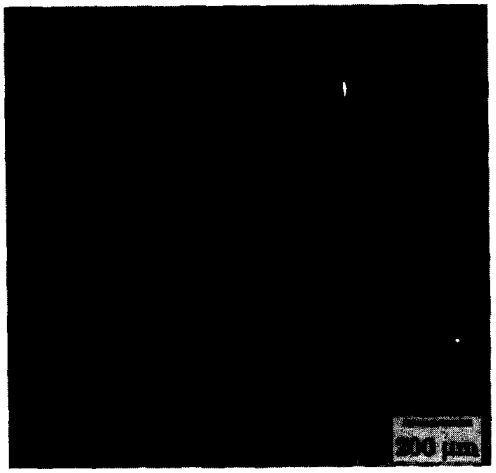

(c) Surface Modified - 4000 cycles

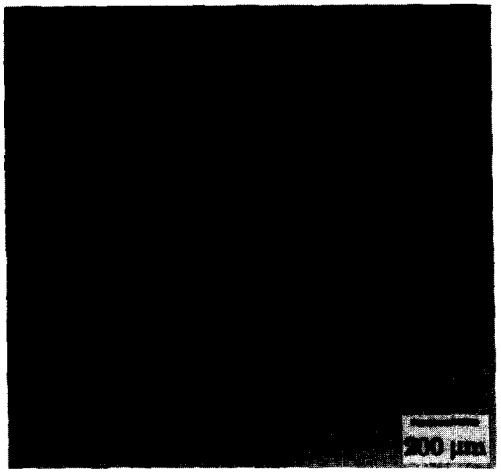

(d) Surface Modified - 40,000 cycles

FIG. 3. Light micrographs of acetate replicas of the surfaces of the unmodified and surface modified specimens after 4000 and 40,000 cycles. The two micrographs of each specimen are from the same area of the specimen surface.

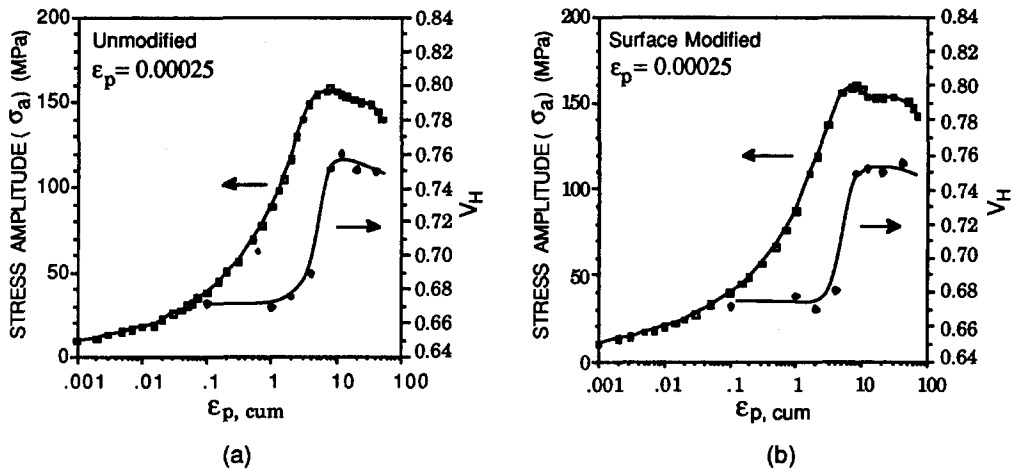

FIG. 4. Cyclic hardening and loop shape parameter curves for (a) unmodified and (b) surface modified polycrystalline nickel fatigue specimens.

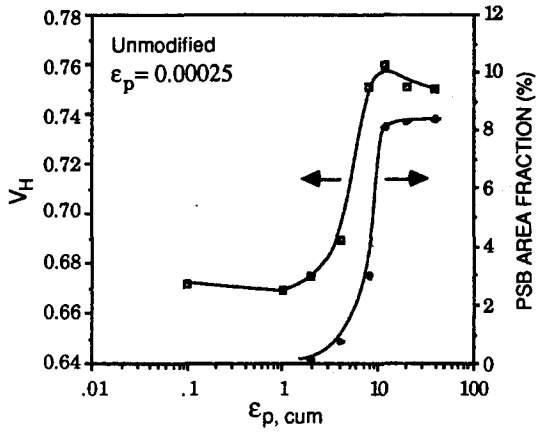

FIG. 5. Loop shape parameter and psb area fraction curves for the unmodified specimen. The psb area fraction was obtained from surface replicas and represents the percentage of the surface area covered by psbs.